OPTIMAL CONTROL OF PENDUBOT SYSTEM USING SIMATIC S7-1200

Van-Dat Nguyen[1]*, Quang-Dong Dang[1], Minh-Tai Vo[2,3], Minh-Duc Tran[2], Anh-Khoa Vo[4], Thanh-Binh Nguyen[5], Phuoc-Tung Tran[5], Huu-Sang Le[5]

[1] Hung Yen University of Technology and Education (UTEHY)
Dan Tien, Khoai Chau District, Hung Yen Province, 16000, Vietnam
[2] Ho Chi Minh city University of Technology (HCMUT), VNU-HCMC
Ly Thuong Kiet St., No. 268, District 10, Ho Chi Minh City, 700000, Vietnam
[3] Royal Melbourne Institute of Technology (RMIT)
Nguyen Van Linh Blvd., No. 702, Tan Hung ward, District 7, HCMC, 700000, Vietnam.
[4] Robert BOSCH Engineering and Business Solutions (BOSCH), Vietnam
Cong Hoa St., No. 364, Tan Binh District, Ho Chi Minh City, 700000, Vietnam
[5] Ho Chi Minh city University of Technology and Education (HCMUTE)
Vo Van Ngan St., No. 01, Thu Duc City, Ho Chi Minh City, 700000, Vietnam

***** Corresponding author. E-mail: datvio204@gmail.com

Abstract: In optimal control, a common problem is developing a control law that can drive a dynamical system from one state to another as quickly as possible. The objective of paper is to design optimal control approach based SIMATIC S7-1200 for under-actuated Pendubot system. The main contribution of this paper is to introduce and validate control method for laboratory model of Pendubot system by using industrial device, namely, Programmable logic controller (PLC). Besides, Lyapunov Analysis is used to analyze the stability of optimal control. The simulation is performed in MATLAB/Simulink environment and experiment is carried out in TIA PORTAL environment. The simulation results and experimental results illustrate that the proposed control method is effective and robust by using PLC.

Keywords: Optimal control, SIMATIC S7-1200, Pendubot, PLC, underactuated system.

1. Introduction

Pendubot is a combination of Pendu (Pendulum) and bot (robot) - an under-actuated system that has fewer control inputs than degrees of freedom, and is difficult to control with nonlinearities. Then, we propose a solution and build LQR controller to control the system. In this paper, the classic LQR controller is embedded in Siemens S7-1200 to control Pendubot system instead of conventional microprocessors. By using an industrial circuit board with high anti-interference ability like PLC, it will pave the way for the research and application of algorithms in the field of automatic control in industry. Moreover, the Pendubot system together with the LQR algorithm will be pre-simulated by MATLAB software to validate the system's response and find the optimal LQR controller parameters.

Currently, the research of control engineering in Vietnam has been promoted a lot. In [1], the fuzzy-sliding control method is applied to the Pendubot system. In addition, the Fuzzy intelligent control algorithm is used to optimize the PID controller applied to the Pendubot system in [2]. Besides, in recent years, the Pendubot system is often selected as a topic for graduation thesis. In [3], the author designs, manufactures and controls the Pendubot system stably. The LQR algorithm is applied to control of the Pendubot system in the graduate thesis [4]. In 1995, Daniel J. Block and Mark W. Spong published a paper on the design and control of the Pendubot system [5]. Up to now, based on the nonlinear structure of this system, there have been many papers developing algorithms to control stability for the system such as linear algorithm LQR [6], sliding algorithm [7], method energy [8], backstepping [9], fuzzy [10], adaptive algorithms to control the system in case of noise and uncertainty components [11], [12], [13].

According to studies on Pendubot, it shows that Pendubot is not a new object and has been exploited a lot by authors. However, most of the literature designs the controller and embeds it in microprocessor boards to control Pendubot. The microprocessor has the advantage of fast processing, but it is susceptible to interference by external factors.

The rest of this paper is organized as follow. First, mathematical model of Pendubot is given and control strategy is described in this section. Then, methodology of optimal control is called back, and stability analysis is carried out for optimal control by using Lyapunov Analysis. In the next section, the simulation results and experimental results are shown to discuss the pros and cons when author uses PLC to control the Pendubot. Finally, the conclusion and final remark are given.

2. Mathematical Model of Pendubot

2.1. Dynamic Analysis

The Pendubot consists of two links linked together by a passive joint as shown in Fig. 1. The bottom of link 1 is attached to active joint, which is the shaft end of the DC motor. Both Pendubot links can rotate freely in the vertical plane.

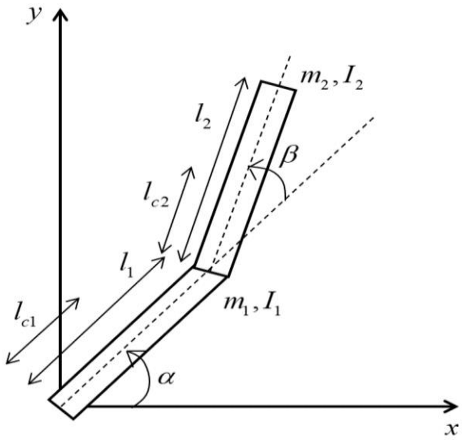

Fig. 1. Pendubot in Cartesian coordinate systems.

System parameters of Pendubot are described in Tab. 1:

Tab. 1 The system parameters of Pendubot.

Nr.	Parameter	Description
1	α	Angle of link 1
2	β	Angle of link 2
3	m_1	Mass of link 1
4	l_1	Length of link 1
5	l_{c1}	Distance from the axis of encoder of link 1 to center of link 1
6	I_1	Inertia moment of link 1
7	m_2	Mass of link 2
8	l_2	Length of link 2
9	l_{c2}	Distance from the axis of encoder of link 1 to center of link 2
10	I_2	Inertia moment of link 2
11	g	Gravitational acceleration
12	K_t	Torque constant
13	K_v	DC motor back emf constant
14	R_a	Resistance

According to [3], equations of motion in matrix form are given by

$$D(q)\ddot{q}+C(q,\dot{q})\dot{q}+G(q)=\tau \tag{1}$$

Where

$$q=\begin{bmatrix}\alpha\\ \beta\end{bmatrix},\ \tau=\begin{bmatrix}\tau_1\\ 0\end{bmatrix} \tag{2}$$

$$D(q)=\begin{bmatrix}\theta_1+\theta_2+ & \theta_2+\\ +2\theta_3\cos\beta & +\theta_3\cos\beta\\ \theta_2+\theta_3\cos\beta & \theta_2\end{bmatrix} \tag{3}$$

$$C(q,\dot{q})=\begin{bmatrix}-\theta_3\sin\beta\dot{\beta} & -\theta_3\sin\beta\dot{\beta}-\theta_3\sin\beta\dot{\alpha}\\ \theta_3\sin\beta\dot{\alpha} & 0\end{bmatrix} \tag{4}$$

$$G(q)=\begin{bmatrix}\theta_4 g\cos\alpha+\theta_5 g\cos(\alpha+\beta)\\ \theta_5 g\cos(\alpha+\beta)\end{bmatrix} \tag{5}$$

$$\begin{cases}\theta_1=m_1{l_{c1}}^2+m_2{l_1}^2+I_1\\ \theta_2=m_2{l_{c2}}^2+I_2\\ \theta_3=m_2l_1l_{c2}\\ \theta_4=m_1l_{c1}+m_2l_1\\ \theta_5=m_2l_{c2}\end{cases} \tag{6}$$

Relationship of torque and voltage is as follows

$$\tau_1=\frac{K_t e}{R_a}-\frac{K_t K_v\dot{\beta}}{R_a} \tag{7}$$

According to (1), we have

$$\begin{bmatrix}\ddot{\alpha}\\ \ddot{\beta}\end{bmatrix}=D^{-1}\left(\begin{bmatrix}\tau_1\\ 0\end{bmatrix}-C\begin{bmatrix}\dot{\alpha}\\ \dot{\beta}\end{bmatrix}-G\right) \tag{8}$$

$$\ddot{\alpha}=\frac{1}{\beta_1\beta_2+\beta_2k_3-{\beta_3}^2\cos^2\beta}[\beta_2k_1e-\beta_3\sin\beta(-\beta_2\dot{\alpha}^2-\beta_3\cos\beta\dot{\alpha}^2-\beta_2\dot{\beta}\dot{\alpha}-\dot{\beta}^2+$$
$$-\dot{\alpha}\beta_2\dot{\beta})-\beta_2k_2\dot{\alpha}-\beta_2\beta_4g\cos\alpha+\beta_3\beta_5g\cos(\alpha+\beta)\cos\beta]$$

$$\ddot{\beta}=\frac{1}{\beta_1\beta_2+\beta_2k_3-{\beta_3}^2\cos^2\beta}[-\beta_2k_1e-\beta_3\cos\beta k_1e \tag{9}$$
$$-((-\beta_3\sin\beta\dot{\beta}+k_2)(-\beta_2-\beta_3\cos\beta)+(\beta_1+\beta_2+2\beta_3\cos\beta+k_3)(\beta_3\sin\beta\dot{\alpha}))\dot{\alpha}$$
$$-(-\beta_2-\beta_3\cos\beta)(-\beta_3\sin\beta)(\dot{\beta}+\dot{\alpha})\dot{\beta}$$
$$-\beta_5g\cos(\alpha+\beta)(\beta_1+\beta_3\cos\beta+k_3)-\beta_4g\cos\alpha(-\beta_2-\beta_3\cos\beta)]$$

After obtaining the differential equation of the system, the state space equation is deduced from the differential equation as follows

$$\begin{cases} \dot{x}(t) = Ax(t) + Bu(t) \\ c(t) = Cx(t) \end{cases} \tag{10}$$

Where

$$x = \begin{bmatrix} \alpha \\ \dot{\alpha} \\ \beta \\ \dot{\beta} \end{bmatrix}$$

$$A = \begin{bmatrix} 0 & 1 & 0 & 0 \\ \frac{\partial \ddot{\alpha}}{\partial \alpha} & \frac{\partial \ddot{\alpha}}{\partial \dot{\alpha}} & \frac{\partial \ddot{\alpha}}{\partial \beta} & \frac{\partial \ddot{\alpha}}{\partial \dot{\beta}} \\ 0 & 0 & 0 & 1 \\ \frac{\partial \ddot{\beta}}{\partial \alpha} & \frac{\partial \ddot{\beta}}{\partial \dot{\alpha}} & \frac{\partial \ddot{\beta}}{\partial \beta} & \frac{\partial \ddot{\beta}}{\partial \dot{\beta}} \end{bmatrix}; \ \mathrm{B} = \begin{bmatrix} 0 \\ \frac{\partial \ddot{\alpha}}{\partial e} \\ 0 \\ \frac{\partial \ddot{\beta}}{\partial e} \end{bmatrix}; \tag{11}$$

$$C = \begin{bmatrix} 1\ 0\ 0\ 0 \\ 0\ 0\ 1\ 0 \end{bmatrix}$$

(With $\alpha = 0$; $\beta = 0$; $\dot{\beta} = 0$; $\dot{\alpha} = 0$; $e = 0$)

2.2. Control Strategy

The Pendubot system has 4 special positions, including 2 stable positions and 2 unstable positions. Figures 2 to 5 show 4 special positions of Pendubot.

We can observe that at angular position $q1 = \frac{-\pi}{2}$, $q2 = 0$ and $q1 = \frac{\pi}{2}$, $q2 = -\pi$ in figures 2 and 3, respectively, Pendubot system is stable naturally.

In figures 4 and 5, the pendubot system is no longer stable. With a minor force from gravity, it is enough to make the system fall down and lose stability. The requirement is to design the controller to keep the system balanced at the MID position (Fig. 4) and the TOP position (Fig. 5). To make the system balance at these positions, the motor needs to rotate with the appropriate voltage and must reverse the direction continuously.

In this manuscript, the TOP position is focued on controlling.

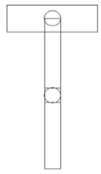

Fig. 2. $\left(\frac{-\pi}{2}; 0\right)$.

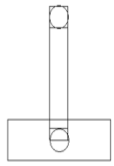

Fig. 3. $\left(\frac{\pi}{2}; -\pi\right)$.

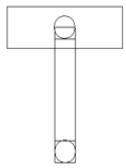

Fig. 4. $\left(\frac{-\pi}{2}; \pi\right)$.

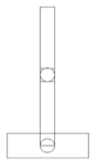

Fig. 5. $\left(\frac{\pi}{2}; 0\right)$.

3. Methodology

3.1. Implementing Optimal Control of Pendubot System

The priciple of LQR control and stability analysis are based on [4]. Controlling Pendubot at TOP position, we set as follows (12):

$$x = \begin{bmatrix} x_1 & x_2 & x_3 & x_4 \end{bmatrix}^T = \begin{bmatrix} \alpha + \frac{\pi}{2} & \dot{\alpha} & \beta & \dot{\beta} \end{bmatrix}^T \tag{12}$$

Accordingly, equations (11) become equations (13), (14) as follows:

$$A = \begin{bmatrix} \frac{\partial f_1}{\partial x_1} & \frac{\partial f_1}{\partial x_2} & \frac{\partial f_1}{\partial x_3} & \frac{\partial f_1}{\partial x_4} \\ \frac{\partial f_2}{\partial x_1} & \frac{\partial f_2}{\partial x_2} & \frac{\partial f_2}{\partial x_3} & \frac{\partial f_2}{\partial x_4} \\ \frac{\partial f_3}{\partial x_1} & \frac{\partial f_3}{\partial x_2} & \frac{\partial f_3}{\partial x_3} & \frac{\partial f_3}{\partial x_4} \\ \frac{\partial f_4}{\partial x_1} & \frac{\partial f_4}{\partial x_2} & \frac{\partial f_4}{\partial x_3} & \frac{\partial f_4}{\partial x_4} \end{bmatrix}; \ \mathrm{B} = \begin{bmatrix} \frac{\partial f_1}{\partial e} \\ \frac{\partial f_2}{\partial e} \\ \frac{\partial f_3}{\partial e} \\ \frac{\partial f_4}{\partial e} \end{bmatrix}; C = \begin{bmatrix} 1\ 0\ 0\ 0 \\ 0\ 0\ 1\ 0 \end{bmatrix} \tag{13}$$

$$f_1(x) = \dot{x}_1 = x_2;$$

$$f_2(x) = \dot{x}_2 = \ddot{x}_1 = \frac{1}{\theta_1\theta_2 + \theta_2 k_3 - \theta_3^2 \cos^2 x_3}[\theta_2 k_1 e - \theta_3 \sin x_3(-\theta_2 x_2^2 - \theta_3 \cos x_3 x_2^2$$

$$-\theta_2 x_4 x_2 - x_4^2 - x_2\theta_2 x_4) - \theta_2 k_2 x_2 - \theta_2\theta_4 g \cos(x_1 + \frac{\pi}{2}) + \theta_3\theta_5 g \cos(x_1 + \frac{\pi}{2} + x_3)\cos x_3)];$$

$$f_3(x)=\dot{x}_3=x_4;$$
$$f_4(x)=\dot{x}_4=\ddot{x}_3=\frac{1}{\theta_1\theta_2+\theta_2k_3-\theta_3^2\cos^2 x_3}[-\theta_2k_1e-\theta_3\cos x_3k_1e$$
$$-((-\theta_3\sin x_3x_4+k_2)(-\theta_2-\theta_3\cos x_3)+(\theta_1+\theta_2+2\theta_3\cos x_3+k_3)(\theta_3\sin x_3x_2))x_2 \quad (14)$$
$$-(-\theta_2-\theta_3\cos x_3)(-\theta_3\sin x_3)(x_4+x_2)x_4$$
$$-\theta_5 g\cos(x_1+\frac{\pi}{2}+x_3)(\theta_1+\theta_3\cos x_3+k_3)-\theta_4 g\cos(x_1+\frac{\pi}{2})(-\theta_2-\theta_3\cos x_3)];$$

3.2. LQR Controller

Control law of LQR technique is given by

$$u(t)=-Kx(t) \quad (15)$$

Where K can be found easily by using MATLAB command K = *lqr(A,B,Q,R)*.

4. Validation

4.1. Simulation Results

The validation is performed in MATLAB environment. There are 3 scenarios with difference starting point were set up for Simulink model. The simulation results are shown from Fig. 6 to Fig. 8. The period time of simulation is 10 seconds. In scenario 1, 2 and 3, the first link and the second link are stable at equilibrium point after 2 seconds. The angular velocity of link 1 and link 2 are stable after 2 seconds. After validating with MATLAB, we observe that the LQR control scheme can achieve the controlled requirement which we defined Section 2.2. We continuously developed LQR controller for experiment setup in Section 4.3.

Parameters of Pendubot are given below:

m_1 = 0.137 kg; l_1 = 0.2 m; l_{c1} = 0.1 m; m_2 = 0.042 kg; l_2 = 0.22 m; l_{c2} = 0.105 m; I_1=0.0017($Kg.m^2$); I_2=0.000148($Kg.m^2$).

Motor's parameters are as given as follows:

K_b=0.065($V/(rad/s)$);
K_t = 0.0108 (Nm/A);
R_a = 6.836 (Ω);
J_m = 0.000134 ($Kg.m^2$);
C_m = 0.000048 ($Nm/(rad/s)$).

The input matrices A and B at TOP position are expressed in Eq. (16) and the weighting matrices Q and R are selected as expressed in Eq. (17)

$$A=\begin{bmatrix}0 & 1 & 0 & 0\\ 43.2628 & -0.1840 & -17.2938 & 0\\ 0 & 0 & 0 & 1\\ -34.9385 & 0.4495 & 112.9764 & 0\end{bmatrix} \quad B=\begin{bmatrix}0\\ 2.6285\\ 0\\ -6.4204\end{bmatrix} \quad (16)$$

$$Q=\begin{bmatrix}1 & 0 & 0 & 0\\ 0 & 1 & 0 & 0\\ 0 & 0 & 1 & 0\\ 0 & 0 & 0 & 1\end{bmatrix};\ R=1. \quad (17)$$

The optimal gain, K is obtained as expressed in Eq. (18).

$$K=\begin{bmatrix}-133.2886 & -25.8219 & -136.9279 & -15.5378\end{bmatrix} \quad (18)$$

Scenario 1: $\alpha=-0.1;\ \dot{\alpha}=-0.2;\ \beta=0.1;\ \dot{\beta}=0.3$

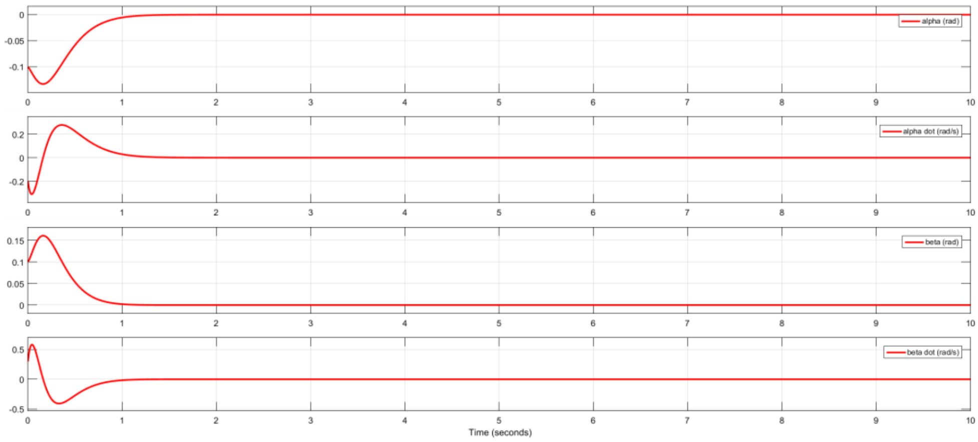

Fig. 6. State responses of system with scenario 1.

Scenario 2: $\alpha = -0.2;\ \dot{\alpha} = -0.05;\ \beta = 0.2;\ \dot{\beta} = -0.3$

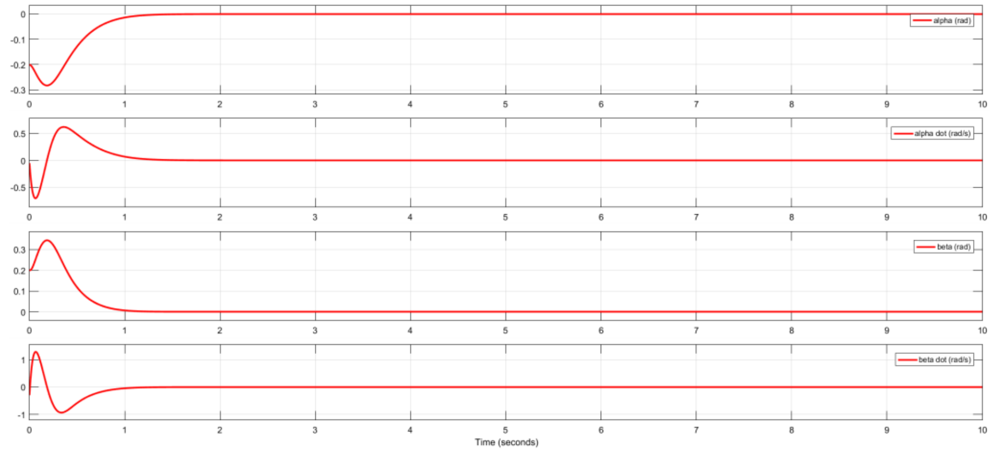

Fig. 7. State responses of system with scenario 2**.**

Scenario 3: $\alpha = 0;\ \dot{\alpha} = 0;\ \beta = -0.5;\ \dot{\beta} = 0$

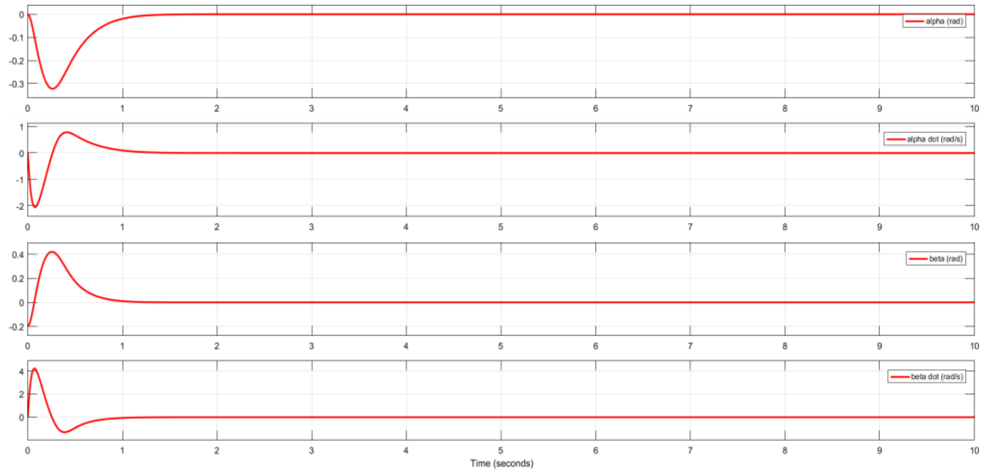

Fig. 8. State responses of system with scenario 3**.**

4.2. System Setup

The experimental setup is designed by SolidWork. Figures 9, 10, 11, 12, 13 show the designation of Pendubot system on SolidWork and in laboratory. PLC S7-1200 and control panel are used in this experiment which are shown in Fig. 14. Driver HÍ6 is used which is shown in Fig. 15. In addition, in this subsection, the connection of PLC and Pendubot diagram, dependency circuits are listed from Fig. 16 to Fig. 19.

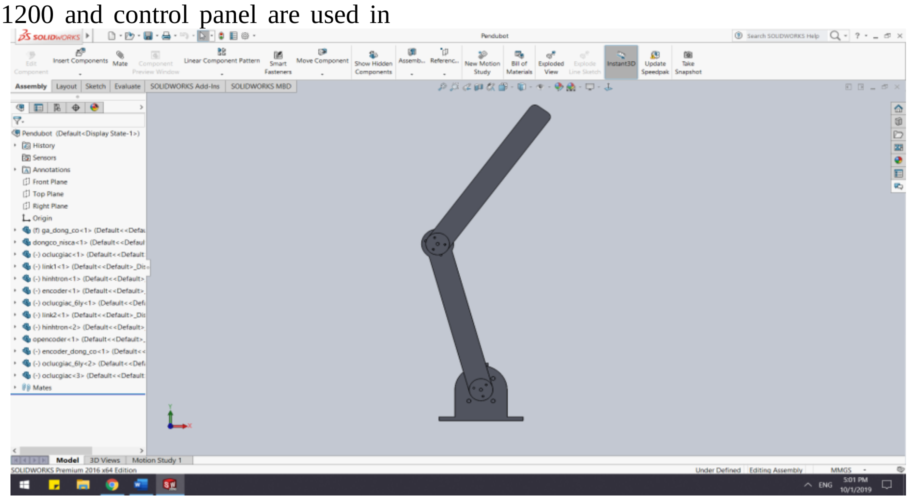

Fig. 9. Front-end of Pendubot**.**

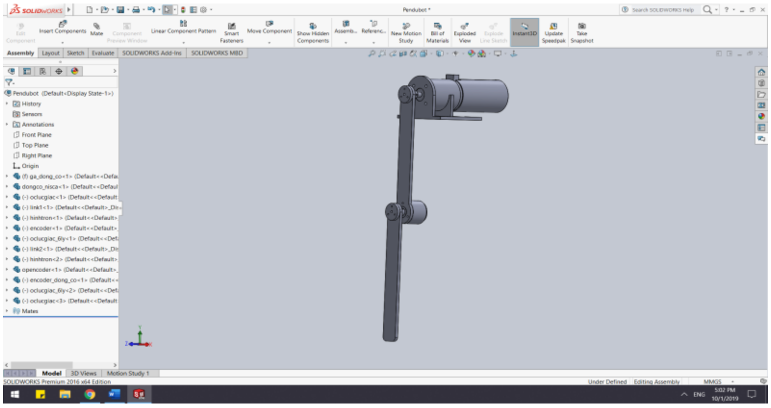

Fig. 10. Pendubot is at BOT position.

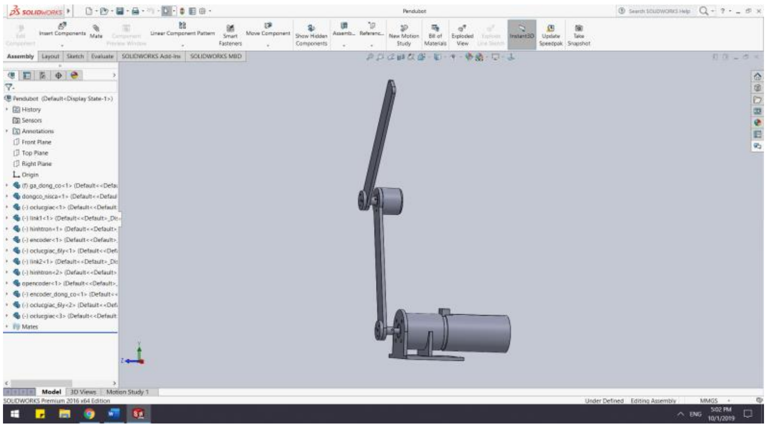

Fig. 11. Pendubot is at TOP position.

Fig. 12. Isometric view of Pendubot.

Fig. 13. Front-end of Pendubot.

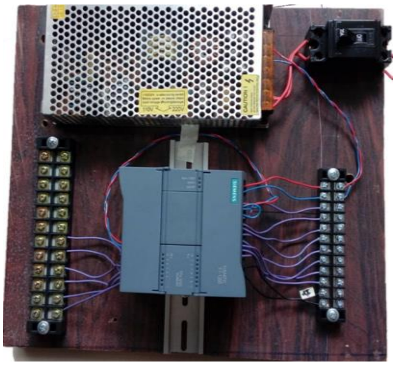

Fig. 14. Control panel PLC S7-1200.

Fig. 15. Driver HI216.

The connection diagram of PLC and Pendubot's components is shown in Figures 16 and 17. The system consists of 4 input signals: phase A, phase B of link 1 and phase A, phase B of link 2. The output uses Q0.0 as PWM pulse output and Q0.1 as signal output (0 or 1) to control the direction of motor rotation.

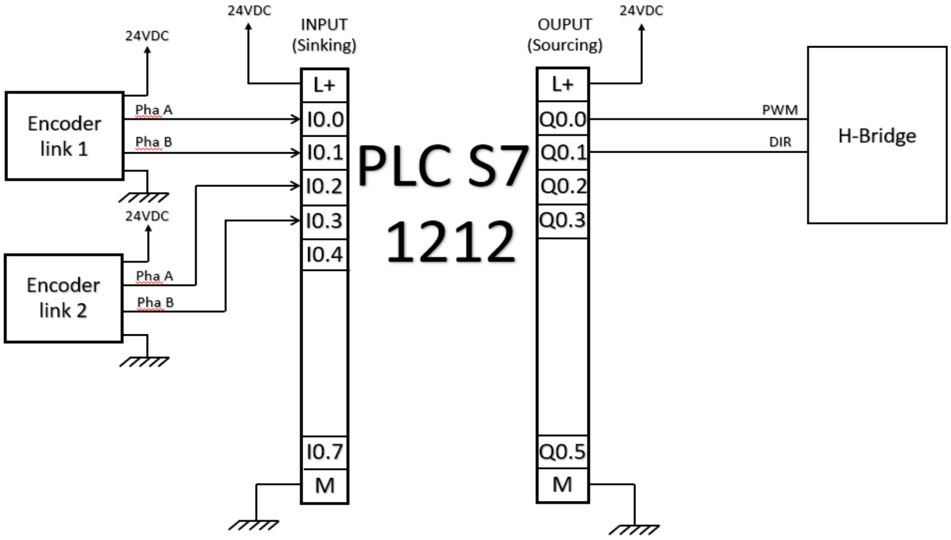

Fig. 16. Connection diagram of PLC and Pendubot's components.

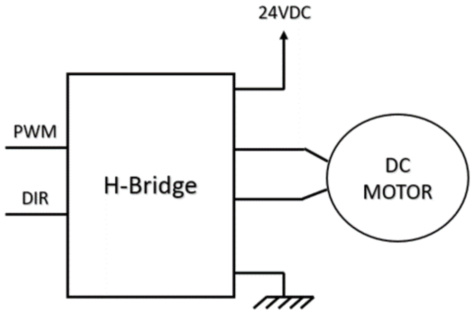

Fig. 17. Power circuit diagram.

The driver's control signal (DIR and PWM pins) requires voltage level from 0-5VDC. However, the output of the PLC has a voltage level of 0-24VDC. Therefore, the 0-24VDC to 0-5V conversion circuit is designed and described in Figures 18 and 19.

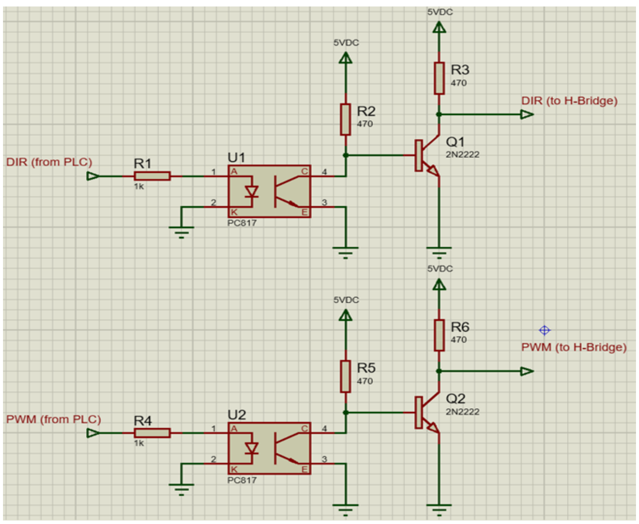

Fig. 18. Design of 0-24 VDC to 5 VDC circuit in Proteus software**.**

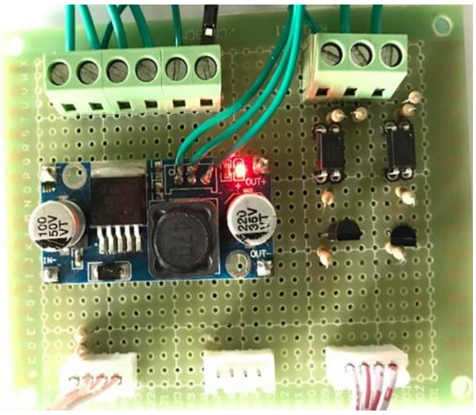

Fig. 19. Design of 0-24 VDC to 5 VDC circuit**.**

4.3. Experimental Results

Based on the successful simulation results, LQR algorithm is programmed to control Pendubot system by PLC S7-1212C.

In the experiment, the system is initially in the BOT position (Fig. 20), then the system is brought to the TOP position (Fig. 21) and the LQR control is used to balance the system in the TOP position. Then, to verify the controllability of the LQR controller, the pendulum is affected by a minor external force at the 9th second, 12th second and 17th second, respectively. The experimental results show that after being impacted, the system quickly returns to the equilibrium point (Fig. 19). The experimental video clip can be watched on YOUTUBE by scanning the QR code in Fig. 22 or via link: https://www.youtube.com/shorts/MR5X4XW3iao. In this video, LQR control scheme is implemented to control Pendubot system in TOP position by using PLC S7-1200. The sample code is used to calculate the angular position of link 1 and link 2 which is captured in Appendix of this paper.

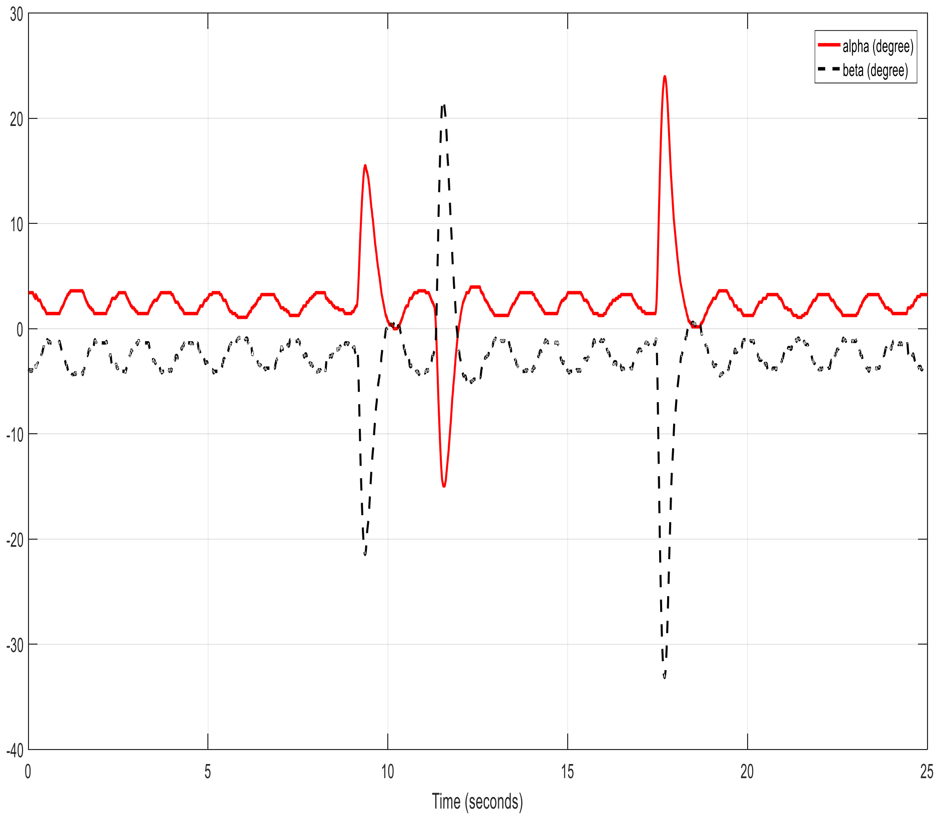

Fig. 19. State responses of experimental setup under LQR**.**

Fig. 20. Pendubot is at BOT position.

Fig. 21. Pendubot is at TOP position under LQR controller.

Fig. 22. QR code for experiment.

5. Conclusions

In this manuscript, the LQR controller has been designed and validated in both simulation and experiment for Pendubot system by using industrial device PLC S7-1200 instead. The state responses in experiment show that the system stabilize at equilibrium point with and without disturbance. However, the controlled parameter of LQR control scheme need to be optimized to control system better. Through this paper, we prove that LQR algorithm can be programmed and validated on the underactuated system such as Pendubot.

6. Appendix

In this section, calculation of angle of link 1 and link 2 are provived.

Calculation of angle of link 1

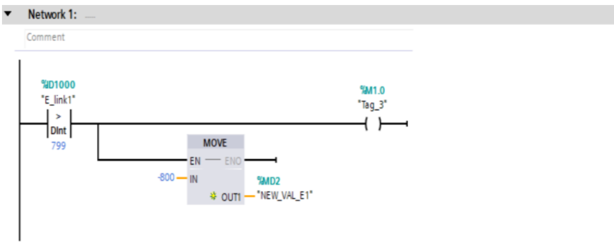

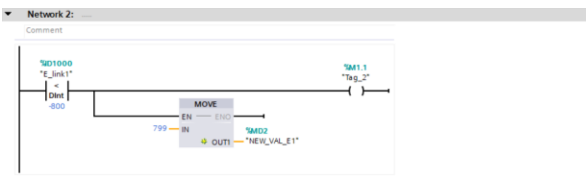

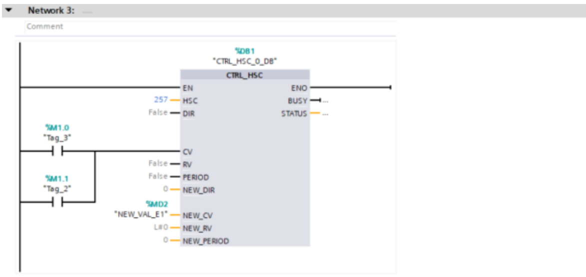

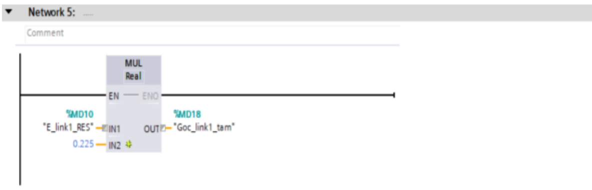

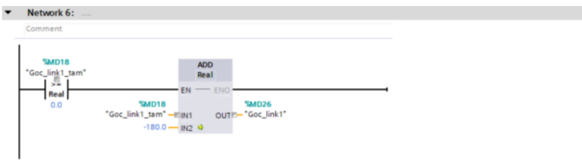

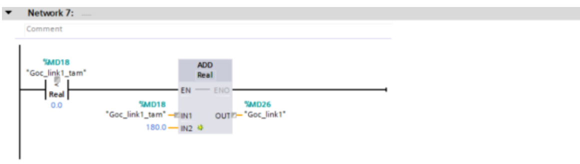

Calculation of angle of link 2

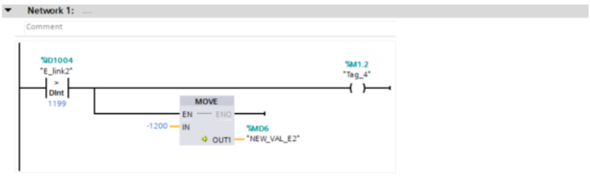

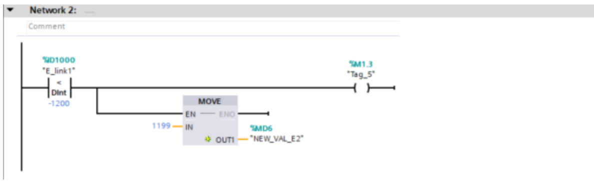

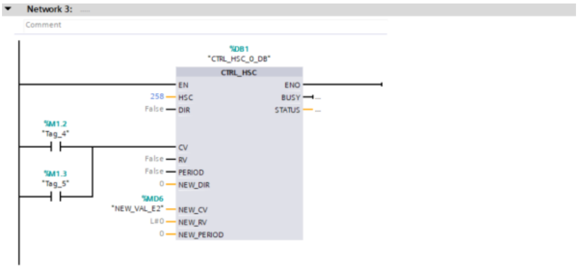

7. References

[1] Vu D.D., Huynh X.D.P.V.K., Nguyen M.T., Nguyen V.D.H.: "A Method of Fuzzy-Sliding Mode Control for Pendubot Model", The University of Danang - Journal of Science and Technology, vol. 11, No. 120.1, Nov. 2017, pp. 12-16, https://jst-ud.vn/jst-ud/article/view/3846.

[2] Tran H.C., Nguyen M.T., Nguyen V.D.H.: "Application of pid-fuzzy control for pendubot", JTE, No. 44A, pp. 61–67, Oct. 2017, https://jte.hcmute.edu.vn/index.php/jte/article/view/379.

[3] Tran V.D.: "Thiết kế chế tạo và điều khiển ổn định hệ Pendubot", School-level scientific research project, 2015.

[4] Pham V.L.: "Điều khiển cân bằng Pendubot", Master thesis at HCMC University of Technology and Education, 2016.

[5] Block D., Spong M.: "Mechanical Design and Control of the Pendubot", SAE Technical Paper 951199, 1995, https://doi.org/10.4271/951199.

[6] Xu J., Huzhen S.: "The Study on PenduBot Control Linear Quadratic Regulator and Particle Swarm Optimization." J. Digit. Inf. Manag, Vol. 11, pp. 16-24, 2013.

[7] Djamila Z., Khier B.: "Optimal sliding mode control of the Pendubot", Journal of Computer Science and Information Systems, Vol. 2, pp. 45-51, 2013.

[8] Fantoni I., Lozano R., Spong M.W.: "Energy based control of the Pendubot", IEEE Transactions on Automatic Control, Vol. 45(4), pp. 725-729, 2000, DOI: 10.1109/9.847110.

[9] Rudra S., Barai R.K.: "Design of block backstepping based nonlinear state feedback controller for Pendubot", 2016 IEEE First International Conference on Control, Measurement and Instrumentation (CMI), pp. 1-5, 2016, DOI: 10.1109/CMI.2016.7413794.

[10] Ma X.Q., Su C.Y.: "Theory and implementation of a fuzzy control scheme for Pendubot", IFAC Proceedings Volumes, Vol.35(1), pp. 335-340, 2002, https://doi.org/10.3182/20020721-6-ES 1901.00868.

[11] Melin P., Castillo O.: "A New Method for Adaptive Control of Non-Linear Plants Using Type-2 Fuzzy Logic and Neural Networks", International Journal of General Systems, Vol. 33, pp. 289-304, 2007, https://doi.org/10.1080/03081070310001633608.

[12] Xia D., Chai T., Wang L.: "Fuzzy Neural Network Friction Compensation-Based Singularity Avoidance Energy Swing-Up to Nonequilibrium Unstable Position Control of Pendubot", Vol. 22(2), pp. 690-705, 2014, DOI: 10.1109/TCST.2013.2255290.

[13] Shibli M.: "Direct Adaptive Control for Underactuated Mechatronic Systems using Fuzzy Systems and Neural Networks: A Pendubot Case", 2006 Canadian Conference on Electrical and Computer Engineering, pp. 1490-1493, 2006, DOI: 10.1109/CCECE.2006.277489.